Towards Commercialization of Perovskite Solar Cells: Fabrication, Lifetime, and Lead Toxicity

Jiarong Liu[1, a, *, †], Yuwen Peng[2, b, *, †], Yiheng Yan[3, c, *, †], Bike Zhang[4, d, *, †]

[1]Faculty of Photovoltaic, University of New South Wales, Kensington, NSW 2052, Australia

[2]Department of Electrical & Electronic Engineering, The University of Manchester, Manchester M13 9PL, UK

[3]Department of Chemistry, The Pennsylvania State University, State College, PA, 16802, United States

[4]Faculty of Applied Science, University of British Columbia, Vancouver, BC, Canada

* Corresponding Author Email: [a*]z5327979@ad.unsw.edu.au, [b*]yuwen.peng@student.manchester.ac.uk, [c*]yxy181@psu.edu, [d*]zhangbik@student.ubc.ca

[†]These authors contributed equally

Abstract. Perovskite solar cells (PSCs) have seen rapid improvement in efficiency recently. As of 2021, the record efficiency is 25.5% and is increasing at a rate of 1% per year. This efficiency is comparable to that of crystalline silicon solar cells. Moreover, PSCs can be prepared using an inexpensive solution process. These two factors give PSCs great potential for revolutionizing the photovoltaics industry. However, most PSCs have a small cell area (~0.1 cm^2), short lifetime (~1000 h), and contain lead, which is toxic to the human body. These factors hinder the market prospect of PSCs. In this work, we reviewed the recent progress towards the commercialization of PSCs. First, fabrication methods able to prepare large-area, high-quality perovskite film are summarized. Then, we discussed methods to improve the lifetime of PSCs in both ideal and actual environments, emphasizing encapsulation techniques. Finally, we reviewed the various approaches to fabricate stable, high-efficiency lead-free PSCs.

Keywords: Perovskite, commercialization, fabrication, lifetime, Lead toxicity

1. Introduction

Technology development to convert renewable energy into electricity is critical for human progress. As of 2015, crystalline silicon solar cells (69.5 percent), multi-crystalline silicon solar cells (23.9 percent), and CdTe solar cells (6.6 percent) were the most extensively commercialized solar cells [1]. These solar modules have certified power conversion efficiencies (PCE) of 27.6 percent for single crystalline silicon, 23.3 percent for multi-crystalline silicon, and 22.1 percent for CdTe, respectively (Fig.1) [2]. We must either lower the present solar cell technology cost or create new photovoltaic technologies to fully utilize abundant solar energy [3].

PSCs have shown exceptional performance, with PCEs as high as 25.5 percent and potential efficiencies as high as 31 percent (Fig.1) [4]. Because of its low cost of raw materials, it is considered to have great potential to be marketable.

Unfortunately, when compared to silicon solar cells, obtaining a satisfactory lifetime during PSC operation is difficult. PSCs are currently only stable for less than one year in an outdoor environment [5]. Almost all PSCs are still under experimental conditions and have not been commercialized, so the fabrication method of large-scale manufacturing still needs further research. Plenty of PSCs contain toxic metals (Pb^{2+}) and halogenates (I^-, Cl^-, Br^-), and how to reduce their impact on the environment is also very important. Several fundamental challenges must be addressed to commercialize PSC technology shortly: (1) Controllable stability and degradation to improve the service life of PSCs. (2) Large-scale fabrication strategy and (3) Low-toxic. In order to commercialize PSCs in the future, the current problems and some recent approaches of these three main challenges are presented in this review.

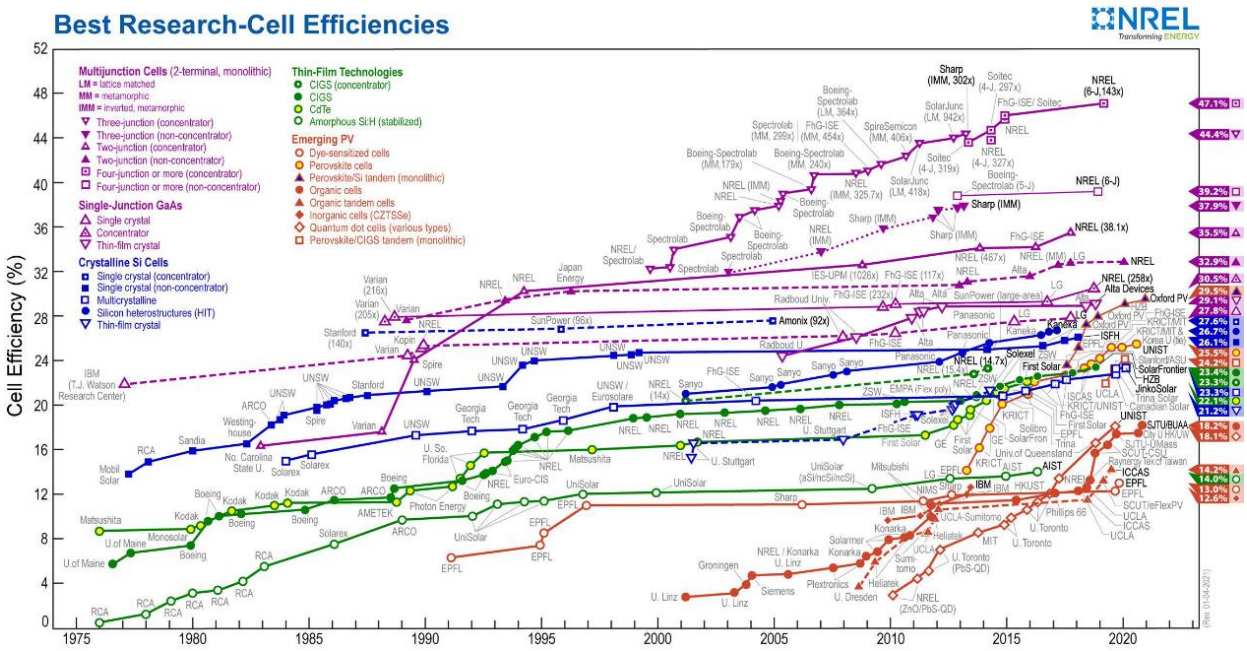

Fig. 1 Best Research-Cell Efficiencies certified by National Renewable Energy Laboratory (NREL) [2]

2. Fabrication

With the improvements in raw material, fabrication process and forming methods to a high-quality film, the power conversion efficiency (PCE) of a small area single PSC has reached 25.5%, which is as high as silicon solar cell. Thus, research on PSCs has opened the door to large-scale production, which means that finding a low-cost and high-efficiency method to prepare large-area film is the point [6]. The prerequisite of improving the quality and performance of devices is to obtain a uniform, dense and pinhole-free calcium titanium deposition. Furthermore, the quality of perovskite film is controlled by the compatibility and controllability of fabricating methods, which ensures that quality in different positions and batches of the same large-area perovskite film is well-consistent. It will enable these preparation technologies to be applied in large-scale production.

At present, the reported fabrication methods of large-area perovskite films include spin coating, spray coating, Doctor-blading, screen printing, slod-die coating, softcover deposition, vapor deposition method and so on. The significant basis for developing large-area perovskite film preparation technology is to understand the complex nucleation thermodynamics and crystal growth kinetics of perovskite films, which will directly affect the technical route and deposition scheme of the large-area perovskite film preparing process. In this section, the preparation technology of perovskite films will be studied from the aspects of material utilization, the basic principle of film-forming, and device performances, which is aimed at better understanding the film-forming mechanism, providing theoretical guidance for the preparation of high-quality, large-area perovskite films and high-efficiency large-area PSC modules in the future and promoting the development of photovoltaic technology in perovskite.

2.1. Spin coating

The thickness of the film is greatly dependent on the concentration of the solution as well as the rotating velocity. The volatility of solvents has some influences on the perovskite crystallization process [7-9]. In the one-step film-forming process, a large number of nonpolar anti-solvents, including chlorobenzene, are used to wash away the solvent in the perovskite precursor and then quickly change the concentration of the precursor solution to make the perovskite reach the supersaturated state and precipitate crystal seeds. The crystal seeds gradually grow in the subsequent

annealing process to form a uniform and dense film [8]. Although the one-step film-forming method can realize the crystal growth rate and process through simple solvent engineering, ion doping and temperature control, improve the quality of the film and reduce the generation of defects, there still exist some problems. For example, a large number of toxic solvents will be used in the preparation process, the repeatability of the preparation period is poor, and film quality is often poor, with a high density of pinholes and small grain sizes. It is suggested by Liang PW et al. that it can be controlled by incorporating additives into its precursor solution to modulate thin film formation [10, 11].

The two-step method was first used to fabricate perovskite battery by immersing the substrate with a rotating substrate in an isopropanol solution of CH_3NH_3I, and achieved an efficiency of 14.1% [12]. Later, it was developed into a two-step continuous spin coating method. Through two-step spin coating and then annealing, the perovskite films were further improved [13]. Moreover, the efficiency of perovskite batteries prepared by the two-step method has made breakthroughs continuously. The fabrication of perovskite is divided into two parts. Firstly, lead iodide (PbI_2) is spin-coated on SnO_2 film, and then the solution containing CH_3NH_3I is spin-coated on PbI_2 film and heated at which temperature. The two films are diffused to obtain perovskite film. For polycrystalline films, grain boundaries are a big defect for film quality. One of the best solutions is that larger grains, fewer grain boundaries per unit area. The grain size obtained by the two-step spin coating method is basically in the range of hundreds of nm, even close to 1μm, so the surface of the perovskite film is uniform and highly crystalline [14]. Even though the two-step perovskite films have outstanding film quality and reproducibility, but the film-forming mechanism of the two-step spin coating process is still uncertain. The crystallization kinetics of perovskite can be accurately controlled by decoupling the crystal nucleation and growth process. Therefore, the reproduction rate and quality of perovskite film are excellent.

Recently, it has been shown that many innovative processes have been come up with by researchers in order to improve the quality of the perovskite film and expand the size. The perovskite film quality is improved by doing spin-coating in moderate humidity, followed by a subsequent annealing process [15]. It has been found that more and more solar cell devices tend to use A-site doping strategies. In the adjustment of A-side composition, compared to the double-cation (MA/FA or Cs/FA), the devices fabricated with the three-cation (FA/MA/Cs) component have better luminance stability as well as higher efficiency [16]. Moreover, other innovative processes also exist; for example, the N_2 gas drying method [17] and the vacuum flash drying method [18] further enhance perovskite film quality. During the spin coating, many raw materials and solvents contained in the solution are wasted, which increases the costs. When using the spin-coating method to enlarge solar cell area, performance generally turns out to be reduced significantly [19,20].

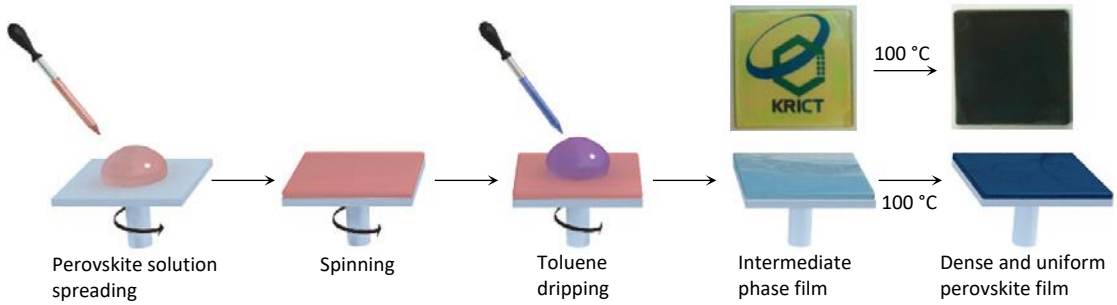

Fig. 2 Processes of spin-coating [21]

2.2. Spray coating

Spray coating is widely used for large-scale, high-throughput fabrication of depositing perovskite films. It is a liquid film deposition technology that applies pressure on the perovskite precursor liquid in the Spray gun to disperse the solution from the nozzle into tiny droplets and uniformly deposit on the substrate. Large area spraying of the perovskite layer is usually based on ultrasonic spraying. In the ultrasonic spraying process, the scattering position of micron precursor droplets is random, so it

is necessary to repeatedly form multilayer droplets superposition in one position to ensure the full coverage of the film. In addition, newly sprayed precursor droplets may dissolve the deposited film during deposition, adding complexity to the process [23]. Therefore, the solvent removal rate and material dissolution are generally controlled by adjusting the volatility of the solvent used in the precursor solution and the corresponding substrate's temperature, inhibiting the redissolution of the deposited material. Therefore, the concentration and viscosity of perovskite solution, base temperature, nozzle diameter and spray flow rate should be considered. Finally, controlling the drying time and annealing conditions is also the key to the deposition of high-quality perovskite films [24]. However, the size and deposition location of droplets in the spray coating is uncertain, which needs to be solved in preparing high-quality perovskite films. In addition, the low raw material utilization rate and part of the escaping toxic liquid are also the disadvantages.

A mono-solvent system of DMSO or DMF and $PbCl_2$ and MAI were used as solutes with this method to achieve 11% PCE and 0.025 cm^2 active area [25]. In addition, a similar process has also been used on a normal structure device that uses TiO_2 as the bottom layer, producing a champion cell and obtain 13% PCE (0.065 cm^2 active area) on a glass/ITO substrate [26]. For a one-step spray deposition process, an active area of 40 cm^2 with 15.5% module efficiency perovskite film was deposited with pure $MAPbI_{3-x}Cl_x$ powder as solutes, DMF and GBL were mixed with a volume ratio of 2:8 as solvent [27].

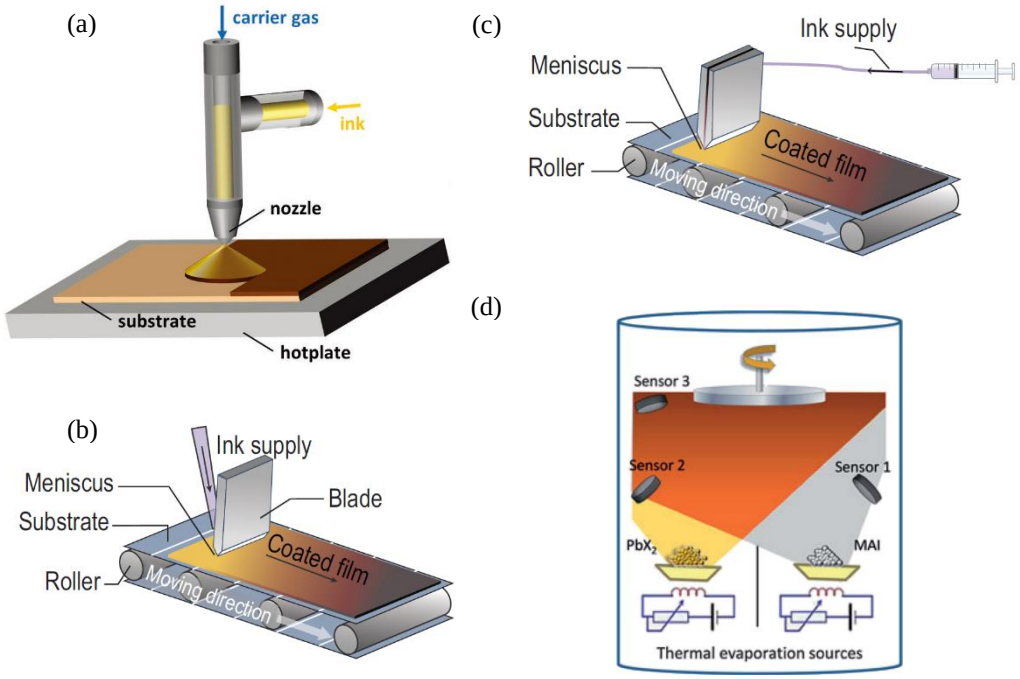

Fig. 3 (a) Spray coating [22]; (b) Doctor-blading [28]; (c) Slot-die coating [28]; (d) Vapor deposition: Schematic diagram of the dual-source vapor deposition process [29].

2.3. Doctor balding

Doctor blading is achieved by the relative movement of scraper and base layer, which means that perovskite precursor solution is painted evenly on the prefabricated base layer using a scraper (Fig.3b) [29-31]. Apparently, the thickness of perovskite film can be controlled by the concentration of precursor solution, gap width between scraper and substrate, scraping speed, and even air knife pressure. Compared with spin coating, the waste of perovskite solution can be greatly reduced when doctor blading is employed. Moreover, doctor balding is superior to spin coating in the film quality and stability of the preparation. Furthermore, doctor blading is similar to split coating in fabrication control.

In the coating process, the perovskite precursor solution will inevitably experience two processes: Landau-Levith and solvent volatilization [30,32]. The Landau-Levich will influence the formation of uniform film and the thickness of perovskite film deposition, increasing as scraping speed increases. Furthermore, in the volatilization process, due to the convective mass transfer effect between the precursor and the medium (such as air or inert gas atmosphere), the thickness of film decreases with the increase of scraping speed [32]. According to the problems in these two processes, many researchers have already prepared a large-area perovskite film by designing a particular precursor ink component. By adding some surface-active agents, for example, L-α-Phosphatidylcholine (LP) in perovskite precursor, the fluid dynamics in the deposition process of perovskite precursor is controlled, which can effectively diminish the effects of the Landau-Levich process. For further slowing the speed of perovskite ink volatilizing in the scarping process, the low vapor pressure solvent N-Methyl-2-Pyr-rolidone (NMP) is used as the solvent of $MAPbI_3$ ink [33].

2.4. Slot-die coating

It is a depositing method that stores perovskite precursor ink in the liquid storage pump and continuously extrudes it from the slit coating head to the substrate through the control system to form a continuous and uniform perovskite liquid film (Fig.3c). This method is a common technology for liquid-phase continuous film making in the industry [34, 35]. There exist several advantages when the slot-die coating method is employed. a) The ideal parameters of perovskite liquid film can be accurately designed by some setting parameters of the control system. For example, the thickness of liquid film deposition can be pre-designed by adjusting gap width between coating head and substrate, substrate moving speed, feeding speed of liquid storage pump and (or) air knife pressure [36, 37]. b) Compared to Doctor blading method, the slot-die coating method is a non-contact liquid film preparation technology, which can avoid direct scratches between the coating head and the substrate due to the poor flatness of the substrate. c) The perovskite precursor will be sealed in a closed reservoir, keeping the precursor concentration constant and reproducibility for laboratories. Furthermore, this will effectively keep researchers away from solvent, which will assure personnel safety [38].

2.5. Vapor deposition

Vapor deposition is a technology for deposition perovskite precursor film by vacuum deposition without using any solvent [39]. It can fabricate large-area perovskite films with high uniformity by precisely controlling the perovskite's stoichiometric ratio during the deposition [40]. A solar cell fabricated with hybrid chemical vapor deposition from Qiu et al. has 9.34% PCE [41]. But the control of vacuum conditions requires an expensive vacuum device and causes the high cost of this method. Then vapor-assisted solution process was developed. Lead halide precursor film is deposited on the substrate by the liquid-phase deposition method and transformed into perovskite film in organic amine halide steam yang. This technology has the advantages of liquid deposition and vacuum deposition, allowing high uniformity perovskite film production with low cost. And the schematic diagram of the dual-source vapor deposition process is shown in Fig.3d. As shown in Fig.3d, heating methylammonium iodide (MAI) in the vacuum leads to a broader evaporating cone, which affects the reading of all sensors [42].

3. Lifetime

Although the PCEs of PSCs are improving at a rate of approximately 1.44% per year from 2013 to 2020, the lifetime is still insufficient for commercial use (Fig.1).

What is the solar module or panel lifetime? A 20 percent drop in initial performance is one of the most used definitions for solar module/panel failure in photovoltaic technology (relative degradation), also known as the T80 [43]. In order to make solar cells commercially competitive with other forms of electricity generation, the Levelized Cost of Electricity (LCOE) is a crucial metric. The LCOE is

expected to be reduced from 9.0 cents/kWh in 2020 to 5.0 cents/kWh for residential by 2030 [44]. Thus, to attain a suitably low LCOE, at least a 20-year lifetime of the PSCs is required.

To better determine the lifetime of each type of solar cell, there are a number of established testing standards for evaluating the stability of solar cells. The IEC 61215 standard is the most relevant industry-standard released by the International Electrotechnical Commission (IEC). IEC 61215 offers a series of rigorous and sequential stress tests that provide accelerated aging circumstances to evaluate the potential lifetime of solar cells in real-world settings. The entire flow is shown in Fig.4 [45].

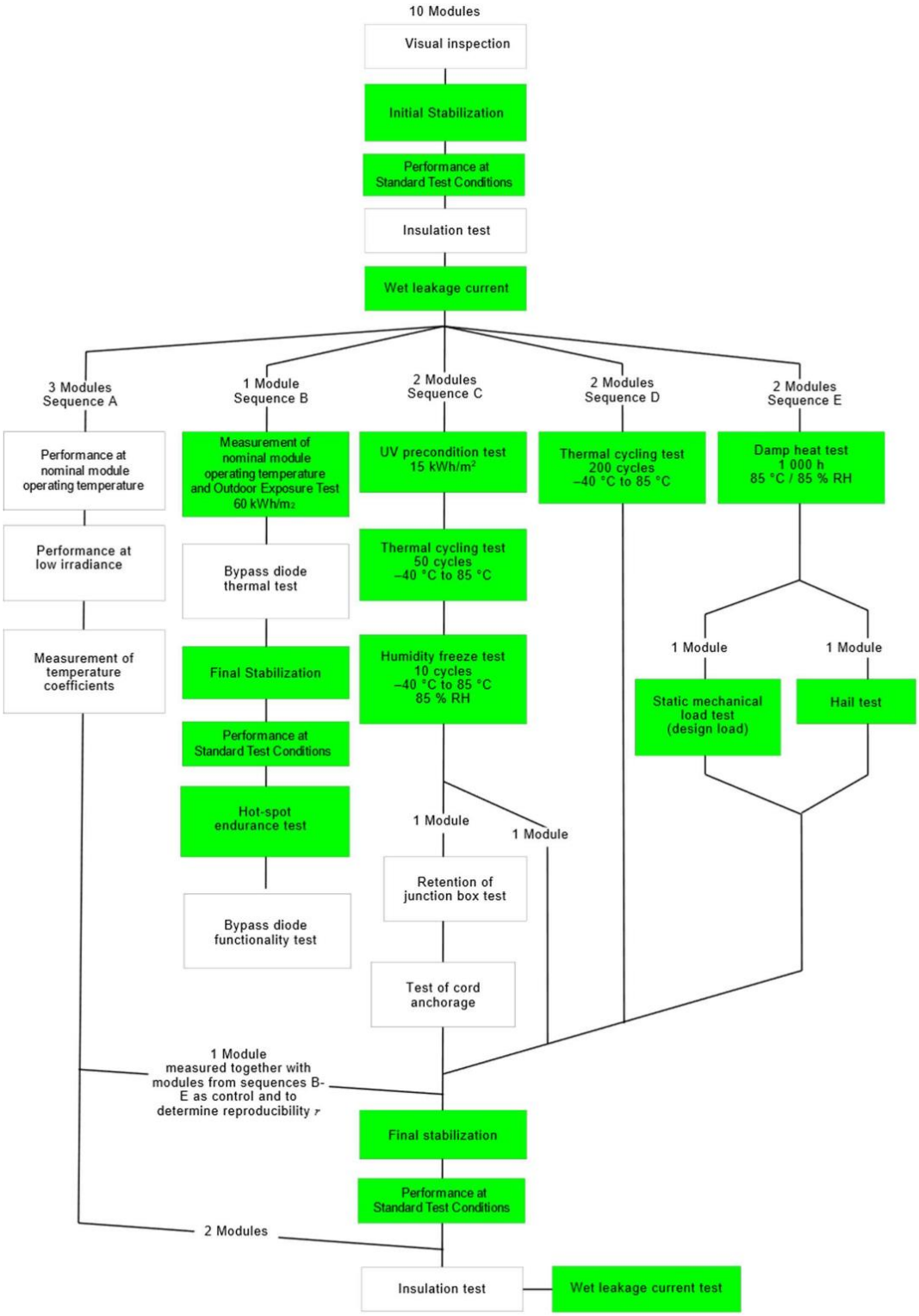

Fig. 4 The entire flowchart of the official module testing for the IEC 61215 standard and the significant PSC stability tests in green [45].

Nevertheless, based on the summary made by Li et al. [46], the PCE and lifespan of PSCs with a service life over 1000h (Table.1) follow the IEC 61215 standard. It is found that the longest lifetime is merely one year [47]. PSCs have a much shorter lifespan than other solar cells because organic-inorganic PSMs can easily degrade under various conditions and PSCs are not robust enough. The ambient environment, as well as layers adjacent to the perovskite, cause stability issues in PSCs. The oxygen, humidity, heat, and illumination all affect the perovskite layer. Therefore, the short lifetime is becoming a major obstacle to commercialization at present [48].

Table 1. The summary of PSCs with service lifetime over 1000h

Device structure	Additives	Modification method	Encapsulation	Test conditions	Lifetime	Ref.
ITO/SnO_2/$Cs_{0.05}FA_{0.54}$-$MA_{0.41}Pb(I_{0.98}Br_{0.02})_3$/spiro-OMeTAD/Au	Fluoride	-	NO	MPP tracking in a nitrogen atmosphere at room temperature under 1-sun illumination (white LED lamp)	1000h with 90% PCE retention	[49]
FTO/NiO/ $(FA_{0.83}MA_{0.17})_{0.95}Cs_{0.05}Pb$-$(I_{0.9}Br_{0.1})_3$/PCBM/BCP /Cr/$Cr_2O_3$/Au	$BMIMBF_4$	-	YES	1-sun illumination under open-circuit conditions at temperatures approximately 70–75 ^oC, RH between 40–60%	1885h with 85% PCE retention	[50]
FTO/SnO_2/C_{60} /$BA_{0.09}(FA_{0.83}Cs_{0.17})_{0.91}$ $Pb(I_{0.6}Br_{0.4})_3$/ spiro-OMeTAD/Au	BA^+	-	YES	Full-spectrum illumination (76 mW cm^2) under open-circuit conditions with RH about 45%	1680h with 80% PCE retention	[51]
FTO/compact TiO_2 /mesoporous/TiO_2 /$(FAPbI_3)_{0.95}$ $(MAPbBr_3)_{0.05}$/ P_3HT/Au	-	Using P_3HT as HTL	YES	MPP tracking at room temperature under 1-sun illumination	1370h with 95% PCE retention	[52]
ITO/$MAPbI_3$/C_{60}/BCP/Ag	-	HTL free	YES	MPP tracking at about 35^oC under 1-sun illumination	1300h with 80% PCE retention	[53]
FTO/TiO_2/ZrO_2 /$(5\text{-}AVA)_x(MA)_{1-x}PbI_3$/C	-	Using carbon electrode	NO	Under 1-sun illumination in ambient air	1008h with 100% PCE retention	[54]
FTO/TiO_2/ZrO_2 /$(AVA)_2PbI_4$/ $MAPbI_3$/C	-	Using carbon electrode	YES	Under 1-sun illumination and short circuit conditions in ambient air at a cycling temperature from 35 to 90 ^oC	10000h with 100% PCE retention	[47]

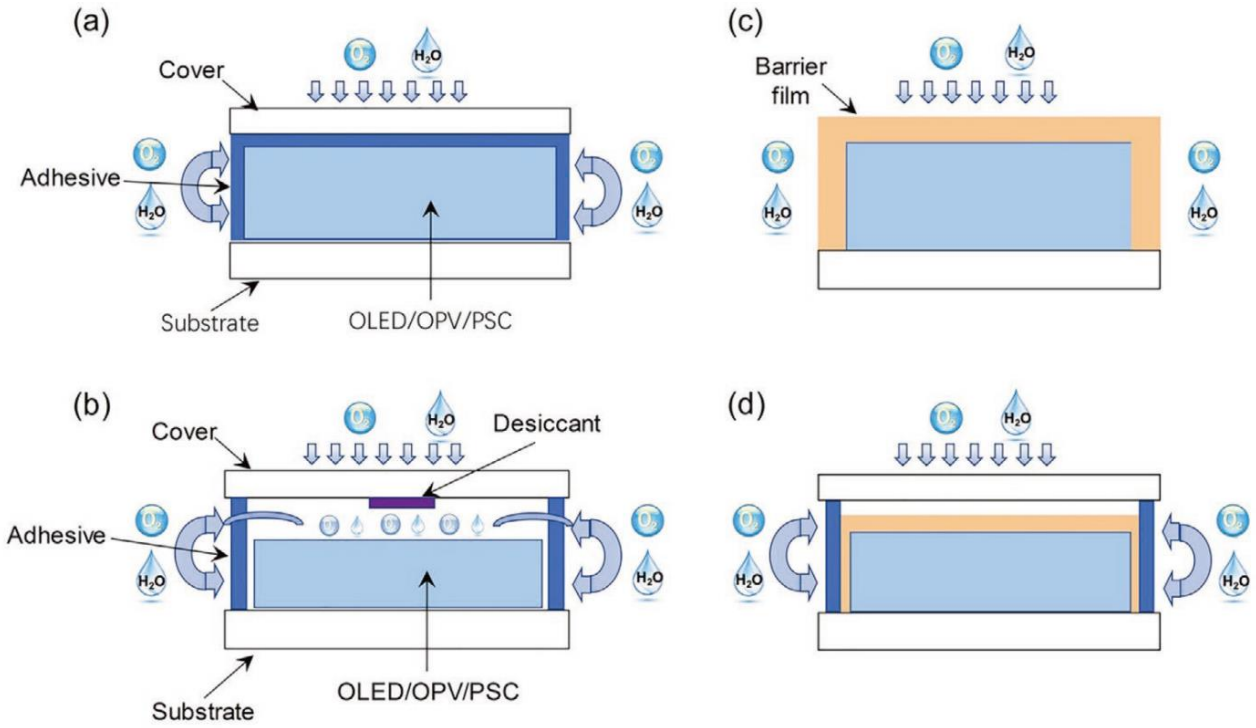

Fig. 5 Schematic diagram of various encapsulation structures. (a) Edged-glass-to-glass encapsulation, (b) Full-glass-to-glass encapsulation, (c) Film encapsulation, (d) Polymer encapsulation [56].

Recent research by Li et al. confirmed that encapsulation is the most critical in improving the stability of PSCs that meet some IEC standards. It acts as a barrier to prevent moisture intrusion into PSCs as well as the leaking of volatile components during decomposition, which will be mentioned in section 3 as well [46]. Next, the three most common encapsulation techniques are briefly described.

So far, various methods for encapsulating PSCs have been developed, including Glass-to-Glass Encapsulation, Polymer Encapsulation, and Thin-Film Encapsulation, which are used to improve the lifetime of PSCs and prevent Pb leakage [55].

One of the most common methods is using thermo-curable or UV-curable sealants based on glass-glass encapsulation to clamp PSC devices on two glasses [57]. In addition, edge sealants can also be used to prevent or at least delay the entry of moisture and oxygen into PSCs from the side circumference to prolong the lifetime of PSCs (Fig.5a and Fig.5b) [58]. Regarding the polymer strategy, it has a wide range of applications in the selection of polymer materials [59].

Thin-film encapsulation (TFE) is one of the most interesting technologies for long-term stable packaging PSCs. It can be done directly on top of perovskite devices by depositing a single film or many layers (Fig.5c) [56]. However, more study is needed to lower the high manufacturing costs, better understand how this encapsulation strategy affects PSC performance, and enhance the long-term stability of encapsulation devices [60]. Finally, the summary of the advantages and challenges of these 3 strategies is displayed in Table.2.

Table 2. The summary of advantages and challenges of 3 main encapsulation strategies

Encapsulation strategies	Advantages	Challenges
Glass-to-Glass Encapsulation	Cost is minimal The simplest process Extremely efficient	It is incompatible with flexible applications, a field that has seen significant growth in recent years.
Polymer Encapsulation	Can be used as a substrate as well as an encapsulating layer Strong Versatility Cost is low Simple process	Poor adhesion [61] High-water vapor transmission rate
Thin-film encapsulation methods	The variety in the deposition technique Thin-film flexibility is combined with the superior barrier qualities of rigid glass coverslips The most promising in terms of technology	High fabrication cost Further research is needed

4. Replacement of Lead

Despite the rapid improvements in PSCs' efficiency and lifetime, most PSCs that excel in these performances contain lead, which is toxic to the human body and may deter public acceptance of PSCs. The situation is exacerbated because lead-based perovskites readily release water-soluble lead halides, such as $PbBr_2$. As mentioned in the previous section, encapsulation is one way to prevent the leakage of lead, but it may increase the cost significantly and thus hinders the commercialization of PSCs. Consequently, it is desirable to develop novel lead-less perovskites or substitute some of the lead with other elements or the so-called "less-lead" perovskites.

Before discussing lead-free perovskite light absorbers, it is necessary to understand the source of the superior performance of lead-based perovskites. Perovskites have a general formula of ABX_3, where A is a univalent cation, usually either of MA (methylammonium), FA (formamidinium), or Cesium ion; B is a bivalent metal ion; X is a halide anion. A occupies the octahedral vacancies in the corner-sharing BX_6 network (See Fig.6a). Theoretical studies [62] have shown that the desirable properties of lead-based perovskites come from their highly symmetrical 3D crystal structure that facilitates charge transfer, as well as special electronic properties of Pb^{2+}. It is commonly believed that the ionic radii of A, B, and X of a Goldschmidt tolerant factor (GTF) t ($t=(R_A+R_B)/[\sqrt{2}(R_B+R_X)]$) between 0.8 and 1 is necessary for a stable, highly symmetrical 3D perovskite structure. The closer GTF is to unity; the higher is the tendency to form a highly symmetrical cubic structure [63]. Nevertheless, Travis et al. [64] pointed out that GTF failed to predict the stability of 32 known iodine perovskites, and we shall later demonstrate how certain desirable properties can be acquired via breaking the GTF rule. On the other hand, the $6s^2$ electrons in Pb^{2+} hybridize with iodine 5p electrons, giving rise to enhanced Born effective charges, which increase the dielectric constant and thus reduce recombination [65]. Therefore, to develop a high-performance lead-free perovskite light absorber, one needs to tune the mean ion radii of A, B, and X via alloying of different species so that a stable perovskite structure can be achieved; one also needs to ensure that the metal ion has ns^2 ($n>3$) lone pair, as it can hybridize with p orbitals of halide anions.

4.1. Tin-Based Perovskites, 3-Dimensional

Based on the two criteria mentioned above, tin is a good replacement for lead, as both lead and tin belong to group 14, wherein Sn^{2+} has $5s^2$ electrons that can hybridize with halides. Additionally, Sn^{2+} and Pb^{2+} have similar ionic radii (1.35 Å vs. 1.49 Å). Ge^{2+}, Sb^{3+}, and Bi^{3+} also have ns^2 electrons, Ge^{2+} is too unstable, and the latter two cannot form neutral perovskite unit cells and thus the highly symmetrical 3D crystal structure which gave lead-based perovskite superior optoelectronic properties.

Indeed, Sn^{2+} ion provides better PCE (~10%) [66] than any other metal ions experimented (~2%) [67]. Some theoretical studies predict that tin-based PSCs may have comparable or even better performance than lead-based PSCs, thanks to their smaller bandgap and greater charge mobility [68].

Nevertheless, Sn^{2+} is readily oxidized into Sn^{4+} in air, losing the crucial $5s^2$ lone pair, whereas Pb^{2+} is stable due to the relativistic $6s^2$ effect. Moreover, oxidation of Sn^{2+} creates holes that recombine with photoelectrons, decreasing V_{OC} (open-circuit voltage) and thus PCE [63]. This means tin-based PSCs have an intrinsically shorter lifetime than lead-based ones. One way to suppress the oxidation of Sn^{2+} is to add extra Sn^{2+} and/or reductants, such as hypophosphorous acid or hydrazine (Table.3). On the other hand, that Sn^{2+} is prone to oxidation also means a broken tin-based PSC poses no environmental hazard, as the oxidation product SnO_2 is harmless.

Another disadvantage of tin-based perovskites is that they crystallize much more quickly from solution than lead-based perovskites, resulting in pinholes on the PSC, decreasing PCE. This problem was addressed by Kanatzidis et al. [69]; their research showed that uniform $MASnI_3$ film could be obtained from dimethyl sulfoxide (DMSO) or N-methyl-2-pyrrolidone (NMP) solutions due to the formation of SnI_2-solvent adduct, which slowed crystallization. Owing to the lack of pinholes as shunt pathways, the PSC reached an unprecedented J_{SC} (short-circuit current density) of 21.4 mA/cm^2.

One important approach to improve tin-based perovskites is A-site engineering, i.e., tuning the crystal structure via altering the composition of A-site cations [67,71,72-78]. As shown in Fig.6b to Fig.6d, as the effective radius of A-cation increases and GTF becomes closer to unity, the crystal structure with enhanced symmetry approaching perfect cubic, which has the best optoelectronic properties. Since $MASnI_3$ and $FASnI_3$ have GTF of 0.94 and 1.02, respectively [63], it is desirable to mix the two cations to create $FA_{0.75}MA_{0.25}SnI_3$, which has GTF very close to unity. Huang et al. fabricated such PSC and reached a PCE of 8.12 %. For comparison, the highest PCE achieved at the time using pure A-site cation tin-based perovskite was 6.22% [78]. The mixed-cation cell boasted a V_{OC} of 0.61 V, which is the highest among tin-based PSC at the time, indicating that cation mixing reduces recombination. Similarly, Wu et al. [72] first mixed cesium ion (which is smaller than MA) with FA to form $Cs_{0.08}FA_{0.92}SnI_3$ and reached a PCE of 6.08%. This PSC showed great stability towards light, heat, and oxygen. Particularly, it retained 90% of its PCE after being stored in nitrogen for 2000 h. Finally, another cation that was mixed with FA is guanidinium (GA), a triammonium. Although GA is slightly larger than FA (GTF of $GASnI_3$ is 1.05), surprisingly, no phase separation was observed when 1 mol% $EDAI_2$ (ethylenediammonium diiodide) was added, suggesting the lattice had simply become larger instead of been distorted. The resulting PSC was stable under one sun illumination and 50% relative humidity for 1 h without significant loss of PCE. Interestingly, the PCE of the champion device using $GA_{0.2}FA_{0.78}SnI_3$- 1% $EDAI_2$ increased from 8.5% to 9.6% after storing in nitrogen for 2000 h, which is one of the highest PCE reported for a tin-based PSC so far. The authors suggested that this is due to the zero-dipole GA retarding oxidation of Sn^{2+} in the presence of moisture [66].

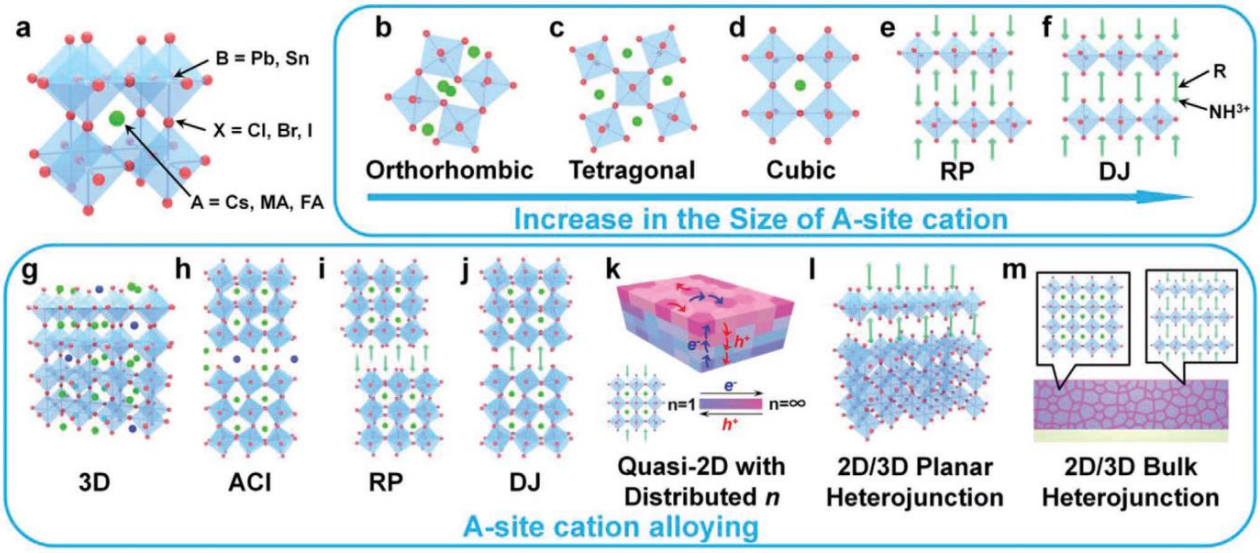

Fig. 6 a) Typical crystal structure of ABX_3 MHPs with ideal cubic phase. ABX_3 structure evolution with increased size of A-site cation: b) Orthorhombic phase, c) Tetragonal phase, d) Cubic phase, e) Ruddlesden-Popper (RP) phase, and f) Dion-Jacobson (DJ) phase. ABX_3 structure evolution with A-site cation alloying: g) 3D, h) ACI, i) RP, j) DJ, k) Quasi-2D with distributed n, l) 2D/3D planar heterojunction, and m) 2D/3D bulk heterojunction. Reproduced with permission from ref [70]. Copyright 2020 John Wiley and Sons.

4.2. Tin-based Perovskites, Quasi-2D

Besides tuning their 3D crystal structure, another approach to improve the performance of PSCs is to mix 2D perovskites with 3D perovskites. As illustrated in Fig.6e to Fig.6f, when A-cation is too large and GTF is much greater than unity, layers of corner-sharing BX_6 networks are cleaved into 2D structure. In 2D perovskites, the large, hydrophobic A-cation encapsulates the BX_6 layers, making 2D perovskites very tolerant towards moisture and oxygen. However, pure 2D perovskites have poor performance due to their low symmetry and thus carrier mobility, as well as the high exciton binding energy due to quantum confinement [80]. Therefore, it is desirable to mix large and small A-cations in the resulting perovskite structure so that each slab of corner-sharing BX_6 contains more than one layer. This structure is known as a quasi-2D structure. In this way, one can improve the optoelectronic properties of 2D perovskites while preserving their stability.

Quasi-2D structures have three types. Note that in DJ phase, A' is divalent. Usually, the inter-layer distance in the RP phase is the greatest, then DJ, then ACI [63]. Since greater inter-layer distance enhances quantum confinement and weakens inter-layer interactions, it is expected that ACI and DJ phases should have better charge mobility, smaller bandgap, and better stability compared to RP phase.

Kanatzidis et al. [73] fabricated the first tin-based quasi-2D PSC, $BA_2MA_{n-1}SnI_{3n+1}$, (BA=butylammonium) which is in RP phase. They showed that, as n increased from 1 to ∞ (i.e., 3D $MASnI_3$), the bandgap decreased from 1.83 eV to 1.20 eV, as quantum confinement became weaker. A maximum PCE of 2.53% was obtained at n=4. Thanks to its 2D structure, the device encapsulated can retain 90% of its PCE after a month. It is worth noting that, in this system, solvent composition determined the orientation of the 2D slabs: when DMSO was used, the resulting slabs were parallel to the substrate; when DMF (N, N-dimethylformamide) was used, the slabs were perpendicular. It was hypothesized that perpendicular slabs benefit charge transfer across the perovskite film, as the spacers themselves can impede charge transfer.

Besides RP phase, DJ phase perovskites have also been employed in PSC as well. The first tin-based DJ quasi-2D PSC was reported by Padture et al. [74], using a dication 4-(aminomethyl) piperidinium (4AMP) as a spacer, with a formula of $(4AMP)FA_3Sn_4I_{13}$. The authors noted unusual long photoluminescence (PL) lifetime of 18.56 ns, whereas typical tin-based perovskites are only

about a few nanoseconds. This suggests the lack of $Sn^{4+,}$ which would act as traps of the photoelectrons, indicating that the 4AMP layer protects perovskite from oxygen well. The resulting PSC has PCE of 4.22%, which is lower than that of 3D $FASnI_3$, although the quasi-2D structure gives it better stability. It lost only 9% of PCE after 100 h under one sun illumination in nitrogen at 45°C. Song et al. [75] improved on this work by switching the A'-cation to 1,4-butanediammonium (BEA), resulting in a formula of $(BEA)FA_2Sn_3I_{10}$. Due to the flexible backbone of BEA, the NH3+ groups penetrated deeper into the perovskite layer compared to previous works on DJ perovskites. This penetration was proven to reduce distortion in the crystal structure and lead to better charge mobility. Correspondingly, the authors achieved a PCE of 6.43%, which is higher than the record efficiency of 3D $FASnI_3$, and the device lost only 8% of PCE after storing in nitrogen for 1000 h and only 9% PCE after one sun illumination in nitrogen at 45°C for 200 h.

4.3. Tin-based Perovskites, 2D/3D hybrid

In quasi-2D structures, when n is large (n>8), quasi-2D phases with uniform n cannot form reliably, as their energy of formation is close to that of 3D phase; instead, a mixture of quasi-2D phase and 3D phase is formed. Such morphology is known as 2D/3D hybrid or 2D/3D heterojunction. Unlike quasi-2D structures with small n, quantum confinement is minimal in 2D/3D hybrid, so it can truly claim to have both the stability of 2D structure and charge mobility of 3D structure.

The first 2D/3D hybrid tin-based perovskite was prepared by Ning et al. [76] using PEA as a spacer. The authors found that when 20 mol% of PEAI was added into $FASnI_3$ (corresponding to an effective n of 9), the resulting film exhibited strong and discrete Bragg spots under grazing-incidence wide-angle X-ray scattering (GIWAXS), indicating the layers of perovskites are preferentially oriented perpendicular to the substrate. In contrast, the scattering image of 3D $FASnI_3$ showed regions corresponding to a random distribution of domain orientation, which is detrimental to charge transfer. This difference in morphology was corroborated by scanning electron microscope (SEM) images, where the hybrid film had lower pinhole density and larger grain size. Higher concentration of PEAI was shown to result in inhomogeneity through the thickness of the film due to different solubility of PEAI and FAI, and may also result in worse optoelectronic properties due to the increased fraction of quasi-2D domain. The 20 mol% PEA perovskite, with formula $PEA_2FA_8Sn_9I_{28}$, was fabricated into PSC and achieved PCE of 5.94%. The device lost only 4% of PCE after storing in nitrogen for 100 h.

To improve on this work, Ning et al. [77] showed that adding NH_4SCN as a catalyst can greatly change the crystal structure of the perovskite. GIWAXS image at an incident angle from 0.2° to 2° (X-ray with greater incident angle penetrate deeper into the film) suggested a 2D-quasi-2D-3D hierarchy structure (HSP), where three phases are formed: a single-layer 2D phase at the top; double-layer quasi-2D phase below; and a 3D phase at the bottom of the film. All three layers are parallel to the substrate. The authors proposed that SCN- act as a Lewis base, which reacts with Lewis acid SnI_2 to form $FASnI_{3-x}SCN_{x,}$ which accelerates the crystallization of 3D $FASnI_3$ at the bottom of the film. During the subsequent annealing, $FASnI_{3-x}SCN_x$ reacts with PEAI, releasing HSCN and forming quasi-2D and 2D perovskites on top of the 3D domain. Despite its parallel orientation, the perovskite achieved a remarkable PCE of 9.41%, which is also one of the highest among tin-based PSCs. On the other hand, the parallel 2D layer protects the entirety of 3D phase, whereas a perovskite phase with perpendicular orientation has its side exposed. Therefore, the HSP solar cell had good stability and lost 10% PCE after storing in nitrogen for 600 h.

Table 3. Photovoltaic parameters of various lead-less or less-lead PSCs.

Perovskite (Additive)	**Device Structure***	**V_{OC} (V)**	**J_{SC} (mA cm^{-2})**	**FF (%)****	**PCE (%)**	**Ref.**
Tin, 3-D Structure						
$MASnI_3$ (20 mol% SnF_2)	regular	0.32	21.4	46	3.15	[69]
$FASnI_3$ (10 mol% SnF_2)	inverted	0.47	22.1	60.7	6.22	[78]
$CsSnI_3$ (20 mol% SnF_2, N_2H_4)	regular	0.17	30.8	34.9	1.83	[79]
$FA_{0.75}MA_{0.25}SnI_3$ (10 mol% SnF_2)	inverted	0.61	21.2	62.7	8.12	[71]
$Cs_{0.08}FA_{0.92}SnI_3$	inverted	0.44	20.7	66.7	6.08	[72]
$GA_{0.2}FA_{0.78}SnI_3$-1%$EDAI_2$ (SnF_2)	inverted	0.62	21.2	72.9	9.6	[66]
Tin, Quasi-2D						
$BA_2MA_3Sn_4I_{13}$ (SnF_2, TEP†)	regular	0.23	24.1	45.7	2.53	[73]
(4AMP)$FA_3Sn_4I_{13}$	regular	0.64	14.9	44.3	4.22	[74]
(BEA)$FA_2Sn_3I_{10}$	inverted	0.62	18.8	55	6.43	[75]
Tin, 2D/3D Heterojunction						
$PEA_2FA_8Sn_9I_{28}$	inverted	0.59	14.4	69	5.94	[76]
$PEA_{0.15}FA_{0.85}SnI_3$ (7.5 mol% SnF_2, 5 mol% NH_4SCN)	inverted	0.61	22.0	70.1	9.41	[77]

Note that: *regular and inverted structure refer to n-i-p (FTO/ETM/perovskite/HTM/metal contact) and p-i-n (FTO/HTM/perovskite/ETM/metal contact) architectures, respectively.
**fill factor. Defined as Maximum Power per Area/(J_{SC}*V_{OC}).
†: Triethylphosphine

5. Conclusion

Based on the results and discussions presented above, the conclusions are obtained as below:

(1) Spray coating is suitable for large-scale, high-throughput perovskite thin films fabrication, but it will escape the toxic liquid. Doctor blading is also widely used for forming large-area PSCs. Slot-die coating can accurately control the parameter of PSCs and has high reproducibility of laboratories. It is also can be used for large-area thin films fabrication. Vapor deposition can fabricate large-area perovskite films with high uniformity, but the PEC is lower than other fabrication methods.

(2) It is because PSCs are easy to degrade under various environmental conditions and the instability of PSCs. Encapsulation is the most critical process of improving the stability of PSCs and prevents Pb leakage. The three most common encapsulation techniques are Glass-to-Glass Encapsulation, Polymer Encapsulation, and Thin-Film Encapsulation.

(3) The leakage of Pb is toxic, and the encapsulation will increase the cost. Therefore, tin is a good replacement for Pb for developing novel lead-free perovskites. Tin-based perovskites, double perovskites, and mixed lead-tin perovskites are three common types of developing PSCs.

References

[1] S. Chu, Y. Cui, N. Liu, The path towards sustainable energy, Nat. Mater. 16 (2017) 16e22.

[2] National Renewable Energy Laboratory, Best research-cell efficiencies chart (2020) ; https: / /www.nrel.gov / pv /assets/ pdfs/ best-research-cell efficiencies. 20201105. Pdf.

[3] Y. Lin, B. Chen, F. Zhao, X. Zheng, Y. Deng, Y. Shao, Y. Fang, Y. Bai, C. Wang, J. Huang, Matching charge extraction contact for wide-bandgap PSCs, Adv. Mater. 29 (2017) 1700607

[4] Kojima, A.; Teshima, K.; Shirai, Y.; Miyasaka, T. Organometal halide perovskites as visible-light sensitizers for photovoltaic cells. J. Am. Chem. Soc. 2009, 131, 6050–6051

[5] Velilla, E.; Ramirez, D.; Uribe, J.-I.; Montoya, J.F.; Jaramillo, F. Outdoor performance of perovskite solar technology: Silicon comparison and competitive advantages at different irradiances. Sol. Energy Mater. Sol. Cells 2019, 191, 15–20.

[6] G. E. Eperon, V. M. Burlakov, P. Docampo, A. Goriely and H. J. Snaith, Adv Funct Mater, 2014, 24, 151-157.

[7] DOCAMPO P, BALL J M, DARWICH M, EPERON G E, SNAITH H J. Efficient organometal trihalide perovskite planar-heterojunction solar cells on flexible polymer substrates. Nature Communications, 2013, 4(1): 1−6. DOI: 10.1038/ncomms3761.

[8] Jeon, N., Noh, J., Kim, Y. et al. Solvent engineering for high-performance inorganic–organic hybrid PSCs. Nature Mater 13, 897–903 (2014).

[9] J.H. Heo, D.H. Song, S.H. Im, Planar CH3NH3PbBr3 hybrid solar cells with 10.4% power conversion efficiency, fabricated by controlled crystallization in the spin-coating process, Adv. Mater. 26 (2014) 8179e8183.

[10] P.-W. Liang, C.-Y. Liao, C.-C. Chueh, F. Zuo, S.T. Williams, X.-K. Xin, J. Lin, A.K.Y. Jen, Additive enhanced crystallization of solution-processed perovskite for highly efficient planar-heterojunction solar cells, Adv. Mater. 26 (2014) 3748e3754.

[11] Y. Wu, F. Xie, H. Chen, X. Yang, H. Su, M. Cai, Z. Zhou, T. Noda, L. Han, Thermally stable MAPbI3 PSCs with efficiency of 19.19% and area over 1 cm2 achieved by additive engineering, Adv. Mater. 29 (2017) 1701073.

[12] Liu M Z, Johnston M B, Snaith H J. Efficient planar heterojunction PSCs by vapour deposition. Nature. 2013, 501(7467):395-398.

[13] Chen Q, Zhou H P, Hong Z R, et al. Planar Heterojunction PSCs via Vapor Assisted Solution Process. Journal of the American Chemical Society. 2014, 136(2):622-625.

[14] Kulbak M, Gupta S, Kedem N, et al. Cesium Enhances Long-Term Stability of Lead Bromide Perovskite-Based Solar Cells. Journal of Physical Chemistry Letters. 2016, 7(1):167-172.

[15] H. Zhou, Q. Chen, G. Li, S. Luo, T.-b. Song, H.-S. Duan, Z. Hong, J. You, Y. Liu, Y. Yang, Interface engineering of highly efficient PSCs, Science 345 (2014) 542e546

[16] Saliba M, Matsui T, Seo J Y,et al. Cesium-containing triple cation PSCs: improved stability , reproducibility and high efficiency. Energy & Environmental Science. 2016, 9(6):1989-1997.

[17] B. Conings, A. Babayigit, M.T. Klug, S. Bai, N. Gauquelin, N. Sakai, J.T.- W. Wang, J. Verbeeck, H.-G. Boyen, H.J. Snaith, A universal deposition protocol for planar heterojunction solar cells with high efficiency based on hybrid lead halide perovskite families, Adv. Mater. 28 (2016) 10701e10709.

[18] X. Li, D. Bi, C. Yi, J.D. Decoppet, J. Luo, S.M. Zakeeruddin, A. Hagfeldt, M. Gratzel, A vacuum flash-assisted solution process for high-efficiency large-area PSCs, Science 353 (2016) 58e62.

[19] M. Yang, Y. Zhou, Y. Zeng, C.-S. Jiang, N.P. Padture, K. Zhu, Square-centimeter solution-processed planar CH3NH3PbI3 PSCs with efficiency exceeding 15%, Adv. Mater. 27 (2015) 6363e6370.

[20] B. Ding, Y. Li, S.-Y. Huang, Q.-Q. Chu, C.-X. Li, C.-J. Li, G.-J. Yang, Material nucleation/growth competition tuning towards highly reproducible planar PSCs with efficiency exceeding 20%, J. Mater. Chem. A 5 (2017) 6840-6848.

[21] N.J. Jeon, J.H. Noh, Y.C. Kim, W.S. Yang, S. Ryu, S.I. Seok, Solvent engineering for high-performance inorganic-organic hybrid PSCs, Nat. Mater. 13 (2014) 897e903.

[22] Howard, Ian & Abzieher, Tobias & Hossain, Ihteaz & Eggers, Helge & Schackmar, Fabian & Ternes, Simon & Richards, Bryce & Lemmer, Uli & Paetzold, Ulrich. (2019). Coated and Printed Perovskites for Photovoltaic Applications. Advanced Materials. 31. 10.1002/adma.201806702.

[23] Heo J H, Lee M H, Jang M H, et al. Journal of Materials Chemistry A, 2016,4,17636.

[24] Qiu, Longbin, L. K. Ono, and Y. Qi." Advances and challenges to the commercialization of organic-inorganic halide perovskite solar cell technology." Materials Today Energy 7 (2018):169-189.

[25] A.T. Barrows, A.J. Pearson, C.K. Kwak, A.D.F. Dunbar, A.R. Buckley, D.G. Lidzey, Efficient planar heterojunction mixed-halide PSCs deposited via spray-deposition, Energy Environ. Sci. 7 (2014) 2944e2950.

[26] S. Das, B. Yang, G. Gu, P.C. Joshi, I.N. Ivanov, C.M. Rouleau, T. Aytug, D.B. Geohegan, K. Xiao, High-performance flexible PSCs by using a combination of ultrasonic spray-coating and low thermal budget photonic curing, ACS Photonics 2 (2015) 680e686.

[27] J.H. Heo, M.H. Lee, M.H. Jang, S.H. Im, Highly efficient CH3NH3PbI3xClx mixed halide PSCs prepared by re-dissolution and crystal grain growth via spray coating, J. Mater. Chem. A 4 (2016) 17636e17642.

[28] Yulong Wang, Changyu Duan, Pin Lv, Zhiliang Ku, Jianfeng Lu, Fuzhi Huang, Yi-Bing Cheng, Printing strategies for scaling-up PSCs, National Science Review, Volume 8, Issue 8, August 2021, nwab075, https://doi.org/10.1093/nsr/nwab075

[29] M. Sessolo, C. Momblona, L. Gil-Escrig and H. J. Bolink, *MRS Bull.*, 2015, 40, 660–666.

[30] Deng, Y., Zheng, X., Bai, Y. et al. Surfactant-controlled ink drying enables high-speed deposition of perovskite films for efficient photovoltaic modules. Nat Energy 3, 560–566 (2018).

[31] Yang, M., Li, Z., Reese, M. et al. Perovskite ink with wide processing window for scalable high-efficiency solar cells. Nat Energy 2, 17038 (2017).

[32] Park, NG., Zhu, K. Scalable fabrication and coating methods for PSCs and solar modules. Nat Rev Mater 5, 333–350 (2020).

[33] Z. Yang, C.-C. Chueh, F. Zuo, J.H. Kim, P.-W. Liang, A.K.Y. Jen, High-performance fully printable PSCs via blade-coating technique under the ambient condition, Adv. Energy Mater. 5 (2015) 1500328.

[34] Cotella G, Baker J, Worsley D, et al. Solar Energy Materials and Solar Cells, 2017, 159, 362.

[35] Kim J E, Jung Y S, Heo Y J, et al. Solar Energy Materials and Solar Cells Volume 179, 1 June 2018, Pages 80-86.

[36] Rong Y, Ming Y, Ji W, et al. The Journal of Physical Chemistry Letters, 2018, 9, 2707.

[37] Galagan Y, Di Giacomo F, Gorter H, et al. Advanced Energy Materials, 2018, 8, 1801935.

[38] T. Qin, W. Huang, J.-E. Kim, D. Vak, C. Forsyth, C.R. McNeill, Y.-B. Cheng, Amorphous hole-transporting layer in slot-die coated PSCs, Nano Energy 31 (2017) 210-217.

[39] Leyden M R,Ono L K, Raga S R, et al. Journal of Materials Chemistry A,2014,2,18742.

[40] Leyden M R, Jiang Y, Qi Y. Journal of Materials Chemistry A,2016,4,13125.

[41] Qiu L, He S, Jiang Y, et al. Journal of Materials Chemistry A, 2019,7,6920.

[42] Sessolo M, Momblona C, Gil-Escrig L, Bolink HJ. Photovoltaic devices employing vacuum-deposited perovskite layers. MRS Bulletin. 2015;40(8):660-666

[43] D.C. Jordan, S.R. Kurtz, Photovoltaic Degradation Rates—an Analytical Review. Progress in photovoltaic. Appl. 21 (2013) 12–29.

[44] S. Chu, Y. Cui, N. Liu, The path towards sustainable energy, Nat. Mater. 16, (2017) 16-22.

[45] P. Holzhey and M. Saliba, J. Mater. Chem. A, 2018, 6, 21794–21808.

[46] N. Li, X.Niu, Q. Chen and H. Zhou, Towards commercialization: the operational stability of PSCs, Royal Society of Chemistry

[47] Grancini, G., Roldán-Carmona, C., Zimmermann, I. et al. One-Year stable PSCs by 2D/3D interface engineering. Nat Commun 8, 15684 (2017).

[48] Lim K G, Ji S G, Kim J Y, et al. Effect of Interfacial Layers on the Device Lifetime of PSCs. Small Methods, 2020, 4(8): 2000065.

[49] Li, N., Tao, S., Chen, Y., Niu, X., Onwudinanti, C. K., Hu, C., Qiu, Z., Xu, Z., Zheng, G., Wang, L., Zhang, Y., Li, L., Liu, H., Lun, Y., Hong, J., Wang, X., Liu, Y., Xie, H., Gao, Y., ... Zhou, H. (2019). Cation and anion immobilization through chemical bonding enhancement with fluorides for stable halide PSCs. Nature energy, 4(5), 408-415.

[50] Bai S, Da P, Li C, Wang Z, Yuan Z, Fu F, Kawecki M, Liu X, Sakai N, Wang JT, Huettner S, Buecheler S, Fahlman M, Gao F, Snaith HJ. Planar PSCs with long-term stability using ionic liquid additives. Nature. 2019 Jul;571(7764):245-250.

[51] Wang, Z., Lin, Q., Chmiel, F. et al. Efficient ambient-air-stable solar cells with 2D–3D hetero-structured butylammonium-caesium-formamidinium lead halide perovskites. Nat Energy 2, 17135 (2017).

[52] Jung, E.H., Jeon, N.J., Park, E.Y. et al. Efficient, stable and scalable PSCs using poly(3-hexylthiophene). Nature 567, 511–515 (2019).

[53] Zhou Z, Qiang Z, Sakamaki T, Takei I, Shang R, Nakamura E. Organic/Inorganic Hybrid p-Type Semiconductor Doping Affords Hole Transporting Layer Free Thin-Film PSCs with High Stability. ACS Appl Mater Interfaces. 2019 Jun 26;11(25):22603-22611.

[54] Mei A, Li X, Liu L, Ku Z, Liu T, Rong Y, Xu M, Hu M, Chen J, Yang Y, Grätzel M, Han H. A hole-conductor-free, fully printable mesoscopic perovskite solar cell with high stability. Science. 2014 Jul 18;345(6194):295-8.

[55] Francesca Corsini, Corsini Francesca, Griffini Gianmarco. Recent progress in encapsulation strategies to enhance the stability of organometal halide PSCs. JPhys Energy,2020,2(3).

[56] Lu Qian, et al. "A Review on Encapsulation Technology from Organic Light Emitting Diodes to Organic and PSCs." Advanced Functional Materials 2021, 31(23).

[57] Bush K A et al. 2017 23.6%-efficient monolithic perovskite/Silicon tandem solar cells with improved stability Nat. Energy 2 1–7.

[58] Kempe M D, Dameron A A, Moricone T J and Reese M O 2010 Evaluation and modeling of edge-seal materials for photovoltaic applications 2010 35th IEEE Photovolt Spec Conf. (Honolulu, HI: IEEE) pp 256–61.

[59] Weerasinghe, H.C.; Dkhissi, Y.; Scully, A.D.; Caruso, R.A.; Cheng, Y.-B. Encapsulation for improving the lifetime of flexible PSCs. Nano Energy 2015, 18, 118–125.

[60] Castro-Hermosa S, Lucarelli G, Top M, Fahlteich J and Brown T M 2020 Perovskite photovoltaics on roll-to-roll coated ultra-thin glass as exceptional flexible power-generator for indoors SSRN Electronic J.

[61] Weerasinghe, H.C.; Dkhissi, Y.; Scully, A.D.; Caruso, R.A.; Cheng, Y.-B. Encapsulation for improving the lifetime of flexible PSCs. Nano Energy 2015, 18, 118–125.

[62] Jena AK, Kulkarni A, Miyasaka T. Halide Perovskite Photovoltaics: Background, Status, and Future Prospects. Chem Rev. 2019 Mar 13;119(5):3036-3103.

[63] Xie LQ, Chen L, Nan ZA, Lin HX, Wang T, Zhan DP, Yan JW, Mao BW, Tian ZQ. Understanding the Cubic Phase Stabilization and Crystallization Kinetics in Mixed Cations and Halides Perovskite Single Crystals. J Am Chem Soc. 2017 Mar 8;139(9):3320-3323.

[64] Travis, W., Glover, E., Bronstein, H., Scanlon, D., & Palgrave, R. (2016). On the application of the tolerance factor to inorganic and hybrid halide perovskites: a revised system.. Chemical science, 7 (7), 4548-4556.

[65] Du, Mao-Hua. "Efficient carrier transport in halide perovskites: theoretical perspectives." Journal of Materials Chemistry 2 (2014): 9091-9098.

[66] Jokar, E.; Chien, C.-H.; Tsai, C.-M.; Fathi, A.; Diau, E. W.-G. Adv. Mater. 2019, 2, 1804835. doi: 10.1002/adma.201804835

[67] Boopathi, K. M.; Karuppuswamy, P.; Singh, A.; Hanmandlu, C.; Lin, L.; Abbas, S. A.; Chang, C. C.; Wang, P. C.; Li, G.; Chu, C. W. J. Mater. Chem. A 2017, 5, 20843-20850. doi: 10.1039/C7TA06679A

[68] Konstantakou, M.; Stergiopoulos, T. J. Mater. Chem. A 2017, 23, 11518-11549. doi: 10.1039/C7TA00929A

[69] Hao, F.; Stoumpos, C. C.; Guo, P.; Zhou, N.; Marks, T. J; Chang, R. P. H.; Kanatzidis, M. G. J. Am. Chem. Soc. 2015, 137, 11445−11452. doi: 10.1021/jacs.5b06658

[70] Gao, W.; Chen, C.; Ran, C.; Zheng, H.; Dong, H.; Xia, Y.; Chen, Y.; Huang, W. Adv. Funct. Mater. 2020, 30, 2000794. doi: 10.1002/adfm.202000794

[71] Zhao, Z., Gu, F., Li, Y., Sun, W., Ye, S., Rao, H., … Huang, C. (2017). Mixed-Organic-Cation Tin Iodide for Lead-Free PSCs with an Efficiency of 8.12. Advanced Science, 4(11), 1700204–1700204.

[72] Weiyin Gao, Chenxin Ran, Jingrui Li, Hua Dong, Bo Jiao, Lijun Zhang, Xuguang Lan, Xun Hou, and Zhaoxin Wu. The Journal of Physical Chemistry Letters 2018 9 (24), 6999-7006. DOI: 10.1021/acs.jpclett.8b03194

[73] Cao, D. H., Stoumpos, C. C., Yokoyama, T., Logsdon, J. L., Song, T. B., Farha, O. K., Wasielewski, M. R., Hupp, J. T., & Kanatzidis, M. G. (2017). Thin Films and Solar Cells Based on Semiconducting Two-Dimensional Ruddlesden-Popper (CH3(CH2)3NH3)2(CH3NH3)n-1SnnI3n+1 Perovskites. ACS Energy Letters, 2(5),982-990.

[74] Min Chen, Ming-Gang Ju, Mingyu Hu, Zhenghong Dai, Yue Hu, Yaoguang Rong, Hongwei Han, Xiao Cheng Zeng, Yuanyuan Zhou, and Nitin P. Padturem ACS Energy Letters 2019 4 (1), 276-277

[75] Li, P.; Liu, X.; Zhang, Y.; Liang, C.; Chen, G.; Li, F.; Su, M.; Xing, G.; Tao, X.; Song, Y. Angew. Chem. Int. Ed. 2020, 59, 6909-6914. doi: 10.1002/anie.202000460

[76] Liao Y, Liu H, Zhou W, Yang D, Shang Y, Shi Z, Li B, Jiang X, Zhang L, Quan LN, Quintero-Bermudez R, Sutherland BR, Mi Q, Sargent EH, Ning Z. Highly Oriented Low-Dimensional Tin Halide Perovskites with Enhanced Stability and Photovoltaic Performance. J Am Chem Soc. 2017 May 17;139(19):6693-6699. doi: 10.1021/jacs.7b01815. Epub 2017 May 2. PMID: 28438016.

[77] Wang, F.; Jiang, X.; Chen, H.; Shang, Y.; Liu, H.; Wei, J.; Zhou, W.; He, H.; Liu, W.; Ning, Z. Joule 2018, 2, 2732-2743. doi: 10.1016/j.joule.2018.09.012

[78] Liao W, Zhao D, Yu Y, Grice CR, Wang C, Cimaroli AJ, Schulz P, Meng W, Zhu K, Xiong RG, Yan Y. Lead-Free Inverted Planar Formamidinium Tin Triiodide PSCs Achieving Power Conversion Efficiencies up to 6.22. Adv Mater. 2016 Nov;28(42):9333-9340. doi: 10.1002/adma.201602992. Epub 2016 Aug 29. PMID: 27571446.

[79] Song, T.-B.; Yokoyama, T.; Stoumpos, C. C.; Logsdon, J.; Cao, D. H.; Wasielewski, M. R.; Aramaki, S.; Kanatzidis, M. G. J. Am. Chem. Soc. 2017, 139, 836-842. doi: 10.1021/jacs.6b10734

[80] Li, X., Hoffman, J. M., & Kanatzidis, M. G. (2021). The 2D halide perovskite rulebook: How the spacer influences everything from the structure to optoelectronic device efficiency. Chemical Reviews, 121(4), 2230-2291. https://doi.org/10.1021/acs.chemrev.0c01006